

XIX. Fluid Physics

SPACE SCIENCES DIVISION

N67-29160

A. A Kinetic Collision Model for Gas Mixtures,

M. T. Chahine

1. Introduction

Recent work (Ref. 1) with the Bhatnagar-Gross-Krook (BGK) collision model for one-particle distribution functions (Ref. 2) has raised interest in further extending this theory to multicomponent gas mixtures (Refs. 3-6). In essence, the BGK model equation approximates the Boltzmann collision operator by a relatively simple expression which retains most of the basic characteristic features of the full Boltzmann equation (BE).

In this phase of research, a generalization of the BGK model to gas mixtures has been developed. The resulting kinetic equation: (1) satisfies the laws of conservation of mass, momentum, and energy; and (2) reproduces the same collision frequencies and exchange of momentum and energy as for a gas mixture in which each constituent is composed of hard molecules and is separately in local Maxwellian equilibrium without necessarily being close to equilibrium with the rest of the gas. In the next phase of research, this model will be applied to the study of

the shock-wave flow problem in a binary gas mixture, using an iteration scheme similar to that adopted in Ref. 1.

2. Formulation of the Kinetic Model

To treat the case of mixtures of two particles i and j , we define a distribution function for each species, e.g.,

$$\frac{\partial f_i}{\partial t} = \frac{\delta f_{ii}}{\delta t} + \frac{\delta f_{ij}}{\delta t} \quad (1)$$

where $f_i(\mathbf{V}_i, \mathbf{x}, t)$ is the number of particles of the i th species in the range $d\mathbf{V}_i d\mathbf{x}$ around \mathbf{V}_i and \mathbf{x} . Gross and Krook (Ref. 3) have postulated the following simple expression for the collision terms:

$$\frac{\delta f_{ij}}{\delta t} = n_j A_{ij} (F_{ij} - f_i) \quad (2)$$

with

$$F_{ij} = n_i \left(\frac{m_i}{2\pi k T_{ij}} \right)^{3/2} \exp \left[-\frac{m_i}{2k T_{ij}} (\mathbf{V}_i - \mathbf{U}_{ij})^2 \right]$$

The mass density $m_i n_i$, average velocity U_{ii} , and kinetic temperature T_{ii} are the first moments of the distribution function

$$\begin{bmatrix} m_i n_i \\ n_i U_{ii} \\ 3kT_{ii} \end{bmatrix} = \int f_i \begin{bmatrix} m_i \\ \mathbf{V}_i \\ m_i (\mathbf{V}_i - \mathbf{U}_{ii})^2 \end{bmatrix} d\mathbf{V}_i \quad (3)$$

To complete this system of equations, we need to determine the expressions A_{ij} , U_{ij} , and T_{ij} .

We chose A_{ij} such that the number of collisions of particles of the i th type with others of the j th type is the same as for a mixture of hard molecules whose constituents are separately in local Maxwellian equilibrium. For the hard molecule case, the number of collisions N_{ij} per unit volume and time can be evaluated for $\mathbf{U}_{ii} \times \mathbf{U}_{jj} = 0$ to be

$$N_{ij} = \frac{n_i n_j \sigma_{ij}}{(\pi a)^{1/2}} \left[(1 + 2M^2) \frac{\pi^{1/2} \phi(M)}{2M} + e^{-M^2} \right] \quad (4)$$

where

$$a = \left(\frac{2kT_{ii}}{m_i} + \frac{2kT_{jj}}{m_j} \right)^{-1}$$

$$M = a^{1/2} (U_{jj} - U_{ii})$$

= diffusion Mach number

$$\sigma_{ij} = \pi (r_i + r_j)^2$$

$$= \text{collision cross-section for hard molecules of radii } r_i \text{ and } r_j$$

$$\phi(M) = \text{erf}(M)$$

Equating Eq. (4) with the number given by the model equation, which is $n_i n_j A_{ij}$, we obtain

$$A_{ij} = A_{ji} = \frac{\sigma_{ij}}{(\pi a)^{1/2}} \left[(1 + 2M^2) \frac{\pi^{1/2} \phi(M)}{2M} + e^{-M^2} \right] \quad (5)$$

For the self-collision frequency, $M = 0$, and the above expression reduces to

$$A_{ii} = 2\sigma_{ii} \left(\frac{4kT_{ii}}{\pi m_i} \right)^{1/2} \quad (6)$$

3. Conservation Laws and Relaxation Properties

The model equation directly satisfies the conservation of mass for each constituent, as well as for the whole mixture. The momentum and energy are not instantaneously conserved, since they are exchanged from one species to the other by cross collisions.

The time rate of change of the i th component of momentum resulting from collisions with the j th component is

$$\frac{\partial}{\partial t} (m_i n_i U_{ii}) = m_i \int \mathbf{V}_i \frac{\partial f_i}{\partial t} d\mathbf{V}_i = m_i n_i n_j A_{ij} (U_{ij} - U_{ii}) \quad (7)$$

The conservation of total momentum becomes

$$m_i (U_{ij} - U_{ii}) + m_j (U_{ji} - U_{jj}) = 0 \quad (8)$$

Similarly, the conservation of total energy is

$$\begin{aligned} (T_{ij} - T_{ii}) + (T_{ji} - T_{jj}) + \frac{m_i}{3k} (U_{ij}^2 - U_{ii}^2) \\ + \frac{m_j}{3k} (U_{ji}^2 - U_{jj}^2) = 0 \end{aligned} \quad (9)$$

Eqs. (8) and (9) form a set of four equations with eight unknowns U_{ij} , U_{ji} , T_{ij} , and T_{ji} ; therefore, we need four more independent relationships to complete the system. These additional relationships will be derived from a study of the relaxation properties.

In the case of a mixture of hard molecules where each of the species i and j is in local equilibrium with itself, we can express the time rate of change of momentum and energy as

$$\begin{aligned} \frac{\partial}{\partial t} (m_i n_i U_{ii}) &= \frac{m_i m_j n_i n_j \sigma_{ij}}{(m_i + m_j) (\pi a)^{1/2}} (U_{ij} - U_{ii}) \\ &\times \left[\left(2 + 2M^2 - \frac{1}{2M^2} \right) \frac{\pi^{1/2} \phi(M)}{2M} \right. \\ &\left. + \left(1 + \frac{1}{2M^2} \right) e^{-M^2} \right] \end{aligned} \quad (10)$$

a.d

$$\frac{\partial}{\partial t} \left(\frac{3}{2} n_i k T_{ii} \right) = \frac{4m_i m_j n_i n_j \sigma_{ij}}{(m_i + m_j)^2 (\pi a)^{1/2}} \left\{ k(T_{jj} - T_{ii}) \left[(1 + 2M^2) \frac{\pi^{1/2} \phi(M)}{2M} + e^{-M^2} \right] + \frac{m_j (U_{jj} - U_{ii})}{2} \left[\left(1 + M^2 - \frac{1}{4M^2} \right) \frac{\pi^{1/2} \phi(M)}{2M} + \left(\frac{1}{2} + \frac{1}{4M^2} \right) e^{-M^2} \right] \right\} \quad (11)$$

Equating Eqs. (10) and (11) with their corresponding values for the model, we obtain the additional four relationships. Solution of this system yields

$$U_{ij} = U_{ii} + \alpha \frac{m_j}{(m_i + m_j)} (U_{jj} - U_{ii}) \quad (12)$$

$$T_{ij} = T_{ii} + 2 \frac{m_i m_j}{(m_i + m_j)^2} \left[\frac{4}{3} (T_{jj} - T_{ii}) + \frac{\alpha}{2} (2 - \alpha) \frac{m_j}{3k} (U_{jj} - U_{ii})^2 \right] \quad (13)$$

where

$$\alpha = 1 + \frac{\left(1 - \frac{1}{2M^2} \right) \frac{\pi^{1/2} \phi(M)}{2M} + \frac{1}{2M^2} e^{-M^2}}{(1 + 2M^2) \frac{\pi^{1/2} \phi(M)}{2M} + e^{-M^2}} \quad (14)$$

For $M \rightarrow 0$, $\alpha \approx 4/3$; for $M \rightarrow \pm \infty$, $\alpha \approx 1.0$.

4. Conclusion

The collision model given by Eq. (2) with parameters as defined in Eqs. (3), (5), (6), (12), and (13) forms a closed mathematical system of integro-differential equations which is much simpler than the full BE. The physical implications of the BGK collision operator are rather clear: It assumes that the molecules, say, of the i th constituent emitted into the velocity range dV_i around V_i are the results of self, ii , and cross, ij , collisions. Furthermore, these colliding particles enter the range dV_i with a Maxwellian distribution of velocities centered around average velocities U_{ii} and U_{ij} and with kinetic temperatures T_{ii} and T_{ij} for self collisions and cross collisions, respectively.

B. The Flow Creating a Concentration of Vorticity Over a Stationary Plate, T. Maxworthy

1. Introduction

When examining the interaction of a tornado with the ground, we are interested in the boundary-layer flow created by the tornado and, as it turns out, in the nature of the rotating outer flow itself. In most boundary-layer problems, the latter is assumed to be known; however, in this case, apparently it is not. Several complicated interactions occur: Since the boundary layers formed must have a smaller angular velocity than the outer flow, they cannot support the outer-flow radial pressure gradient, and a radial inflow is formed. As this converging inflow approaches the center of the tornado, it must eventually erupt into an axial flow over some finite radius. This erupting flow must, in turn, interact directly with the outer flow and alter it in some way. As will be shown, the outer flow has an intense, meridional flow in the neighborhood of the intersection between the wall and the center of rotation. This, in turn, interacts with the boundary layer to not only modify it, but to also, in its turn, be modified by the boundary-layer efflux. After many such interactions, this complicated mechanism finally gives the flow which is observed in the laboratory and, hopefully, is present in nature. The many qualitative attempts to understand the phenomena have been reviewed by Fultz (Ref. 7, which also contains an extensive bibliography on the subject). Ingenious solutions to the problem of creating a suitable convergence of vorticity have been demonstrated, and many realistic-looking tornadoes have been produced. Most of the work did not produce any quantitative results, and it is only in the past few years that a few attempts have been made to do so. Most of these have had their origin in trying to understand the "vortex tube," but, because of their special character, they do not seem to have any direct application to our present problem.

The most recent study of the tornado interaction is that of Turner (Ref. 8). He has approximated the convective

driving mechanism of a real tornado by bubbling air, close to the upper surface, into the center of a rotating tank of water. A strong vortex is formed; however, as a model, it suffers from several disadvantages which he well realizes. It is rotating over a rotating surface, which has a strong effect on the nature of the interaction there. Also, it is surrounded by essentially solid-body rotating flow, which has a strong constraining effect on any radial motion. Thus, axial motion is confined to a central upflow and compensating annular downflow just outside of it. Axial flow beyond about two or three core diameters is zero. In a real tornado, it is unclear as to whether the upward mass flow is not redistributed at considerable radial distances, and whether any evidence of downward axial flow just outside of the central core represents only a part of the total upward mass flux right at the center. In fact, in the present case where mass is being introduced with swirl at large radial distances, the boundary-layer flow from large distances, by representing a significant amount of the exit flow, in a very real sense controls the intensity of the vortex. Furthermore, as the present study shows, some doubt must be cast upon the use of the tangential velocity profile (and its associated pressure gradient) as the *only* driving force for the boundary layer. There is even a real question whether boundary-layer theory is ever valid right at the center of rotation. There the flow turns very rapidly, is ejected, and goes through a breakdown process before it forms the core of the vortex, normally seen far above the surface, all within a distance of the order of the boundary-layer thickness!

2. Apparatus and Experimental Technique

The apparatus used, shown in Fig. 1, is similar to many other devices which have been used to look at the "tornado" phenomenon. It consists of a cylindrical, 11-in.-diameter, 6-in.-deep Lucite tank filled with water. A central sink is connected through a pump and flowmeter to three tangential jets arranged around the periphery. (No attempt has yet been made to simulate the thermodynamic processes of a real tornado, and the present arrangement is probably not the optimum one for observing this phenomenon.) To test some simple physical intuitions concerning the flow, another experiment was performed with the same sink and jets in a tank having approximately three times the diameter and the same depth as that shown in Fig. 1.

Two methods were used to observe the flow in both tanks: (1) dye injection into the boundary layer and main flow to obtain qualitative information about the flow pattern, and (2) the "hydrogen bubble" technique to ob-

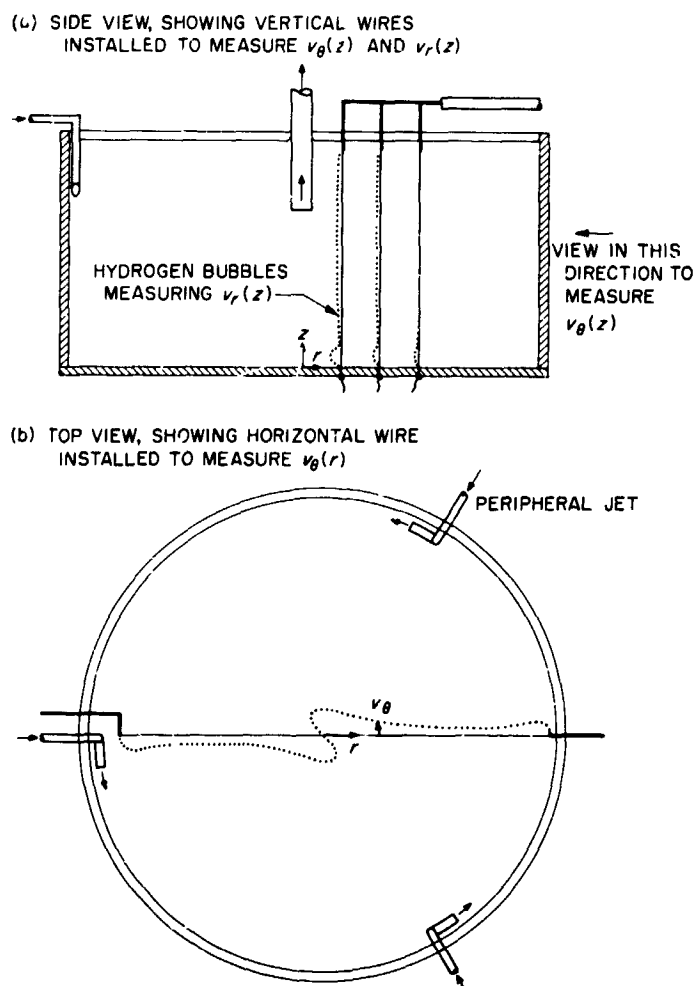


Fig. 1. Apparatus used to investigate the tornado phenomenon

tain quantitative information about the velocity distributions in regions of interest. This has been described in detail by Schraub, *et al.* (Ref. 9). The technique used to measure the radial variation of the tangential velocity, i.e., $v_\theta(r)$ in a cylindrical coordinate system (z, r, θ) , is shown in Fig. 1(b).

In Fig. 1(a), a more complicated geometric situation is shown. Three vertical wires are stretched through the bottom of the tank and are supported, close to the free surface, by 0.040-in.-diameter stainless-steel prongs. By radially viewing these wires and the bubbles produced, we can measure $v_r(z)$; by viewing tangentially, we can measure $v_\theta(z)$ for the three radial locations indicated in the elevation of the apparatus.

3. Results and Discussion

Since most of the experiments were performed in the tank having an 11-in. diameter and a 6-in. depth, only the

exceptions to this case will be noted. Dye injection in various parts of the tank gave the first indication of the nature of the flow field. When dye was introduced through the bottom of the tank into the part of the boundary layer very close to the wall, it moved directly to the center of the tank, was ejected vertically upward, and then spread violently outward to larger radii. After a short axial distance of considerable agitation, a new state was reached, with the dye reappearing at the center of rotation; this state persisted to the exit. Such an ejection and breakup of the dye trace is shown in Fig. 2(a).

If dye was injected further out into the boundary layer, it still moved to the center, but erupted a little before it arrived there; it then wrapped itself around the central stem of Fig. 2(a) into a helix of large pitch angle, at least 45 deg or greater. Anticipating the results of the quantitative velocity measurements to be described, the breakdown, in fact, occurred at the outer limit of the boundary layer. All of the inflowing boundary-layer fluid took part in the breakdown process and was the fluid that eventually made up the central part of the vortex core that was sucked out of the sink tube. This central breakdown¹ has so many of the features of the so-called "vortex break-

¹It appears that this phenomenon has been most convincingly brought to the attention of the scientific community in a film entitled "Secondary Flows in Fluid Mechanics" by E. S. Taylor of the Massachusetts Institute of Technology. Study of several of the very early works on tornado flow reveals that Wilcke (Ref. 13; more recently reported in Ref. 7) was probably the first to observe and sketch the breakdown phenomenon, and that it was rediscovered several times thereafter.

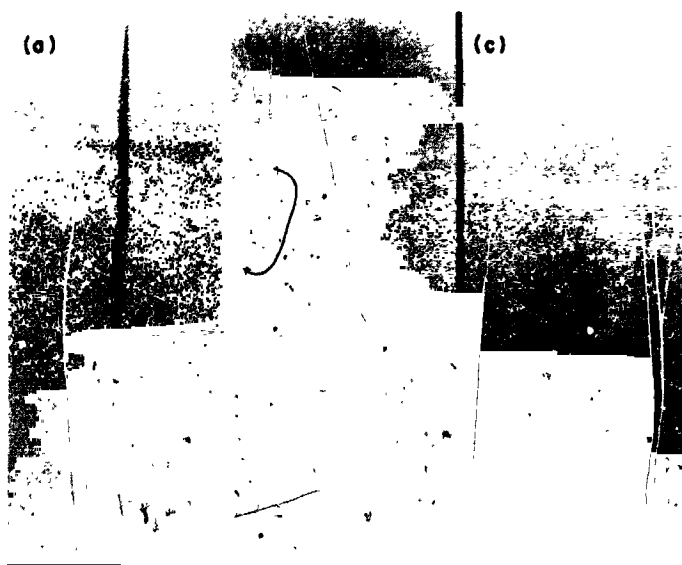


Fig. 2. Vortex breakdown

down" phenomenon [according to Benjamin (Ref. 10) and many others] that it seems certain to be of the same generic type as the disturbances seen by Harvey (Ref. 11), Elle (Ref. 12), and numerous other workers under a variety of circumstances.

As the flow rate (hence, the vortex strength) was increased, the breakdown became more violent (Fig. 2b and 2c) and occurred closer to the wall, since the boundary-layer thickness was decreased, partially in response to the increased velocity of the outer tangential flow. The flow after the breakdown was spread over a larger radius and was mixed with some of the fluid originating from outside the core. The breakdown, if the sink were lowered toward it, could eventually be made to jump inside the tube. If the tube were then raised, the breakdown would move some distance before it would pop out and return to its original position. During this process, the boundary-layer flow and initial supercritical eruption did not change to the accuracy that would enable one to make that determination; the implication here is that, with the tube far removed from the wall, the back pressure is so great that the jump moves as far upstream as it can go, and, as this back resistance is decreased, the breakdown can move downstream to some new position of equilibrium (cf., the behavior of a hydraulic jump as the downstream water height is externally varied).

With the diameter of the sink changed, but at the same high flow rate, the following observations were made: With a 1½-in.-diameter sink, the breakdown occurred and the final diameter of the exit dye column was of the order of the tube diameter; with a ½-in.-diameter tube, the final core flow was reduced in diameter again to the order of the tube diameter; and with a ¼-in.-diameter tube, the core just after the breakdown was still of the order of ½-in. diameter, reducing to ¼-in. as the flow exited through the small pipe. From these tests, it again seems that the flow downstream from the breakdown phenomenon was controlled to some extent by the conditions there; however, the existence of a minimum core size shows that this is not entirely true, and that some dynamic process (presumably viscous forces) becomes important when the velocity gradients tend to become too great.

Having investigated the effects of varying downstream conditions, we turn to the more practically important case of varying the upstream conditions. Because the central core is made up of boundary-layer fluid (probably mixed with fluid from the outside in the case of the more violent breakdowns), it seems probable that a change in the character of the boundary layer will have a considerable effect

on the initial supercritical flow and, hence, on the final subcritical exit flow. These changes can be made in several ways: If a circular wire-screen barrier is placed on the ground around the center of rotation, the boundary layer is forced over and through this resistance. Both angular and radial momentum are changed, and the final vortex flow is considerably weaker than that at the same flow rate but with no barrier. The effect of a simple, circular loop of thick wire, of the same height as the barrier, is not as great, presumably because the angular momentum of the boundary-layer flow is less affected by passing *over* a solid barrier than by passing *through* a stationary, porous screen. However, the most dramatic demonstration of the boundary layer's control over the vortex strength can be made by placing the same jets and sink in a tank having a diameter of 3 ft and a depth of 6 in. At the same flow rate as in the smaller tank, we are introducing about three times the initial angular momentum into the flow; however, since the boundary layer has to flow at least three times farther, the net result is that the vortex strength is considerably reduced, maximum angular velocities being lowered by at least a factor of 5. This great sensitivity to the boundary-layer flow suggests at least one possible means of controlling the growth of a real tornado with the expenditure of a minimum amount of energy. The method can be demonstrated by two more qualitative experiments in widely different pieces of apparatus.

In the present equipment, the introduction of a violent disturbance into the boundary layer, a jet of water from a syringe, destroyed the coherence of an intense vortex for a considerable length of time, although eventually the flow was able to reorganize itself into its original

form. With the "fire-storm" apparatus of Prof. H. W. Emmons at Harvard University, a very large and intense vortex can be created through the induction of an inflow of angular momentum by burning a pool of liquid fuel at the center of a table surrounded by a rotating porous screen. Here again, the character of the vortex can be greatly affected by blowing a puff of air into the boundary layer and upsetting its normal character.

One further dye study gave a qualitative picture of the rest of the flow field outside the boundary layer and the inner region of the concentrated core. For the case of a weak, laminar breakdown, apart from the obvious motion in the boundary layer, several other features of interest were found. The outer region of the concentrated core is made up of fluid that has followed a zig-zag, up-and-down path through the main body of fluid. The up-and-down flows are turned around as they approach the stationary wall and the free surface, where they interacted in some way with the boundary layers on the bottom and the constant pressure surface above. When the intensity of the vortex is increased, the upward and downward flows are also increased in intensity, and the annular region in which they take place decreases in width so that more regions of axial flow occur. Experience in vortex-tube experiments suggests that these regions can become very narrow, and they have been mistaken for evidence of boundary-layer separation. Further discussion on these points will be postponed until more evidence is presented.

Fig. 3 shows a hydrogen-bubble picture of $v_\theta(r)$ at the middle level of the tank and at a known flow rate. This shape persists at all vertical levels (z) above the boundary



Fig. 3. Hydrogen-bubble picture of $v_\theta(r)$

layer to the accuracy of the measurements. This statement is further verified by the shape of the $v_a(z)$ profiles in Fig. 4, which were taken at one radial station. The shape shown in Fig. 3 is characteristic of the $v_a(r)$ profiles for all inlet flow rates. Its most interesting feature is the extensive region of almost constant velocity spanning the annular region between the jets and the sink and a second

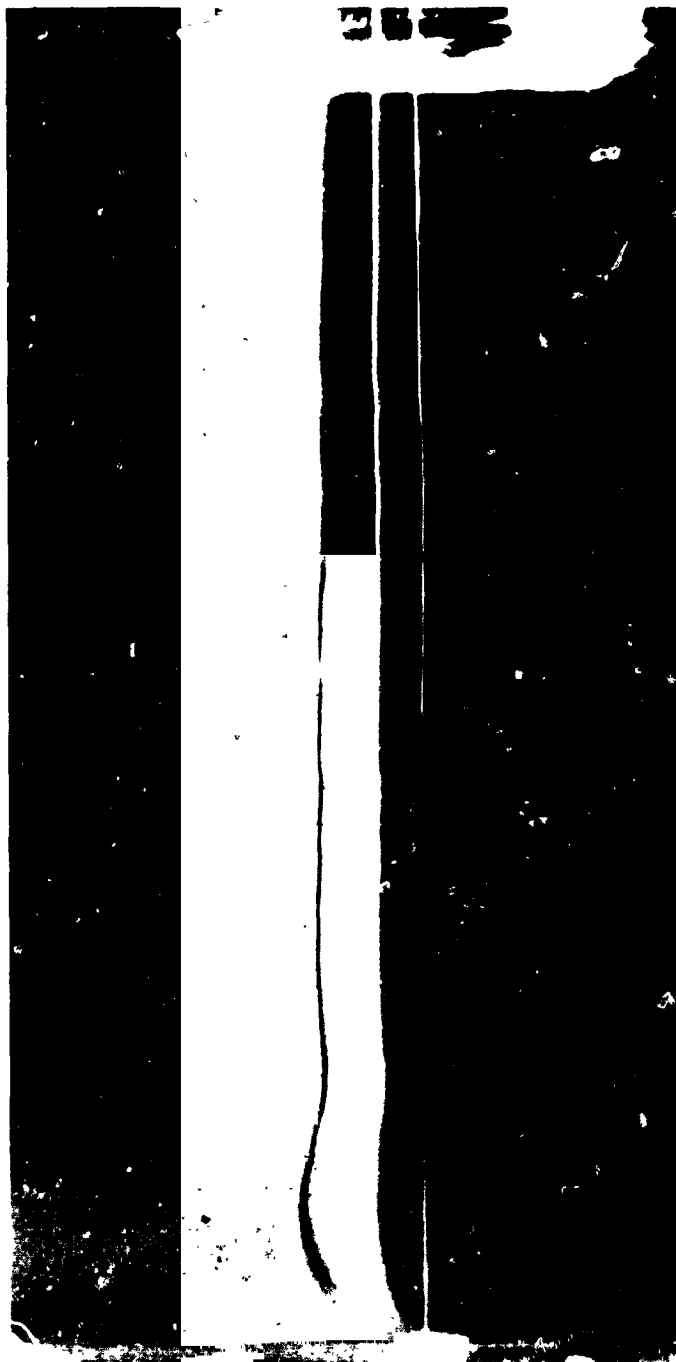


Fig. 4. Hydrogen-bubble picture of $v_a(z)$ at one radial station

maximum in the velocity close to the outer edge of the tank. This is undoubtedly caused by the way we have returned the inlet jet flow to the container; the fluid chooses to return as some form of thick sidewall boundary layer. Since this is only a function of the method, we have chosen to put fluid back into the outer flow and bottom boundary layer; since the flow close to the center is not critically dependent on how this is done, we will ignore further details of this region in what follows.

The most significant calculation we can perform with these profiles is to compute the boundary-layer flow that would be expected with such an outer flow. The most accurate determination of these flows is contained in the extensive work of Mack (Ref. 14) for power-law outer distribution ($v_a \sim r^n$) over a disc of finite radius, and one assumes that the centrifugal pressure gradients of such flows are the driving mechanisms for the boundary layer. Unfortunately, our profiles are not of this simple form, and we are forced to use some more indirect calculation scheme. Rott and Lewellen (Ref. 15) have developed an approximation which depends only on the local values of v_a and r . They assume that the mass flow Q in the boundary layer is a function of the local circulation, $\Gamma = v_a r$, times a universal function of r , which automatically accounts for the boundary-layer history up to the point in question. Thus,

$$\frac{Q}{R_0 (\Gamma_0 v)^{1/2}} = \frac{\Gamma}{\Gamma_0} \left\{ 1.26 \left[1 - \left(\frac{r}{R_0} \right)^{4/3} \right]^{3/4} \right\} \equiv \frac{\Gamma}{\Gamma_0} F \left(\frac{r}{R_0} \right) \quad (1)$$

where R_0 is the outer radius of the disc and Γ_0 is the circulation at that radius. When $\Gamma = \Gamma_0 = \text{constant}$, i.e., a potential vortex, the universal function agrees very closely with the series solution of Mack, and it is possible to replace $F(r/R_0)$ with his more precise calculation. Since $\Gamma_0 = 0$ at R_0 for our flow, we have actually chosen to use the maximum value of Γ to represent Γ_0 , which occurs inside the boundary region on the vertical cylindrical wall. Then, R_0 is the radius at this maximum value of Γ_0 . Calculations based on Eq. (1) and the experimental measurements of $v_a(r)$ are shown in Fig. 5, superposed on Mack's calculated curves. Also shown are experimental measurements of Q based on the $v_a(z)$ profiles found using three vertical hydrogen-bubble wires (Fig. 6). The discrepancies are too startling to be ignored. There are three possible explanations for these differences:

- (1) The theory requires the boundary layer to start with zero thickness and zero mass flow at $r = R_0$, whereas in reality it may have a considerable starting thickness

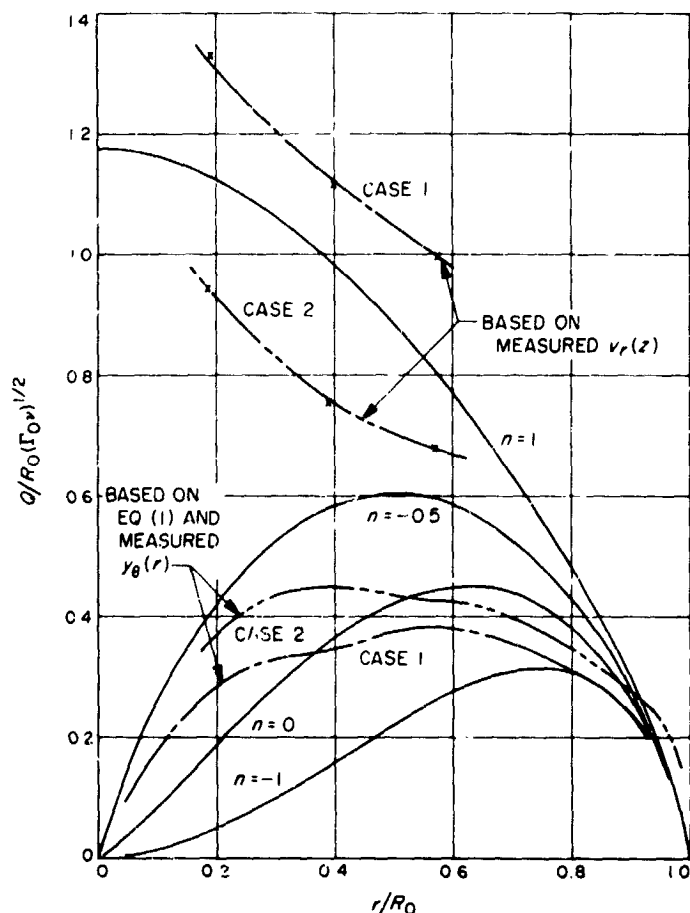


Fig. 5. $Q/R_0 (\Gamma_0 v)^{1/2}$ vs r/R_0

and mass flow. However, this probably does not completely explain the trend of the mass flow with decreasing r . Theory always has Q decreasing in the region of interest (i.e., $r < 7.5$ cm), whereas the experiment shows that Q invariably increases as we approach the concentrated vortex.

(2) This means that more fluid is entering the boundary layer than boundary-layer calculations can allow for, which, in turn, implies that the pressure gradient being imposed on the layer can no longer be solely given by a balance of centrifugal acceleration and pressure gradient in the outer flow. To see that this in fact could be so, we look at the radial equation of motion in the outer flow:

$$-\frac{1}{\rho} \frac{\partial p}{\partial r} = -\frac{v_z^2}{r} + \left(-\frac{v_r^2}{r} + v_z \frac{\partial v_r}{\partial z} - v_r \frac{\partial v_z}{\partial z} \right) \quad (2)$$

All of the extra terms, i.e., those in parentheses above, are known to exist, but experimentally it is hard to determine

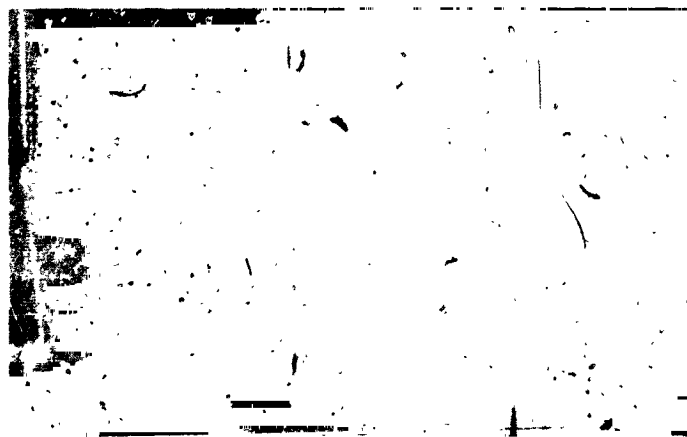


Fig. 6. Hydrogen-bubble picture of $v_r(z)$ at three radial stations

their possible order of magnitude. Observations of the central breakdown region indicate that it has very large axial and radial velocity gradients; e.g., the axial velocity on the centerline changes from a large value, associated with the boundary-layer eruption, to zero after the jump, in a distance of the order of a boundary-layer thickness. Therefore, the terms of Eq. (2), other than v_z^2/r , could combine to increase the outer-flow pressure gradient towards the value for a free vortex, as is required in Case 1.

(3) Since a considerable axial flow is imposed upon the boundary layer, it is also necessary to reexamine the assumptions that have been incorporated into the boundary-layer concept. In the axial equation of motion, it is usually assumed that Δp , the pressure difference across the layer, is small. However, in the present case, we may anticipate that this may no longer be so, since terms like $v_z \Delta v_z$, where Δv_z is the axial velocity difference across the layer, may now become of considerable importance within the layer. Similarly, terms in the equations of motion which are ignored in boundary-layer theory, e.g.,

$$v \left[\frac{\partial^2}{\partial r^2} + \frac{\partial}{\partial r} \left(\frac{1}{r} \right) \right], v_\theta, v_r, v_z$$

may well become overwhelmingly important as $r \rightarrow 0$ for any solution which is not of the similarity type. This means, of course, that conventional boundary-layer theory is no longer valid for these flows, a statement which requires further careful measurements before it can be taken very seriously. These measurements will be reported in future issues of the SPS, Vol. IV.

4. Conclusions

The major results and conclusions can be summarized as follows:

- (1) The tangential velocity profile of the swirling flow of a concentrated laboratory vortex has been measured.
- (2) Boundary-layer flow calculations based on these profiles do not agree with direct measurements of the radial mass flux in the boundary layer.
- (3) This discrepancy can be corrected by allowing for an intense local meridional flow impressed on the boundary layer, in the neighborhood of the axis, which increases the layer's transport of matter.
- (4) In turn, as this boundary-layer material approaches the center of rotation, it erupts to produce this same intense meridional circulation, a "vortex breakdown" similar to the type that described other circumstances (e.g., swirling flow in tubes and flow over delta wings at angle of attack).
- (5) The strength of the vortex is dependent on the history of the boundary layer, thus pointing to possible methods of controlling tornadoes by disturbing the boundary layer at the ground and destroying the tornado's main source of angular momentum.

References

1. Liepmann, H. W., Narasimha, R., and Chahine, M. T., *Physics of Fluids*, Vol. 5, p. 1313, 1962.
2. Bhatnagar, P. L., Gross, E. P., and Krook, M., *Physical Review*, Vol. 94, p. 511, 1954.
3. Gross, E. P., and Krook, M., *Physical Review*, Vol. 102, p. 593, 1956.
4. Sirovich, L., *Physics of Fluids*, Vol. 5, p. 908, 1962.
5. Morse, T. F., *Physics of Fluids*, Vol. 7, p. 2012, 1964.
6. Hamel, B. B., *Physics of Fluids*, Vol. 8, p. 418, 1964.
7. Fultz, D., *Experimental Analogies to Atmospheric Motions*, Compendium of Meteorology, American Meteorological Society of Boston, 1951.
8. Turner, J. S., "The Constraints Imposed on 'Tornado-Like' Vortices by the Top and Bottom Boundary Conditions," *Journal of Fluid Mechanics*, Vol. 25, Part 2, 1966.
9. Schraub, F. A., et al., *Use of Hydrogen Bubbles for Quantitative Determination of the Time Dependent Velocity Fields in Low Speed Water Flows*, Report MD-10, Thermosciences Division, Stanford University, 1964.
10. Benjamin, T. B., "Theory of the Vortex Breakdown Phenomenon," *Journal of Fluid Mechanics*, Vol. 14, Part 4, 1962.
11. Harvey, J. K., "Some Observations of the Vortex Breakdown Phenomenon," *Journal of Fluid Mechanics*, Vol. 14, Part 4, 1962.
12. Elle, B. J., "On the Breakdown at High Incidences of the Leading Edge Vortices on Delta Wings," *Journal of the Royal Aeronautical Society*, Vol. 64, 1960.

References (contd)

13. Wilcke, J. C., "Forsøg til Uplysning om Luft-Hvirflar og Sky-drag," *K. Vet. Acad. nya Handl.*, Vol. 29, 1780.
14. Mack, L. M., *The Laminar Boundary Layer on a Disk of Finite Radius in Rotating Flow*, Technical Report 32-224, Part 1, Jet Propulsion Laboratory, Pasadena, California, 1962.
15. Rott, N., and Lewellen, W. S., "Boundary Layers and Their Interaction in Rotating Flow," *Progress in Aeronautical Sciences*, Vol. 7, 1966.